Molecular Therapy
Oncolytics
Original Article

Regulating Stem Cell-Related Genes Induces the Plastic Differentiation of Cancer Stem Cells to Treat Breast Cancer

Jing-Ying Zhang,[1,2] Qian Luo,[1,2] Jia-Rui Xu,[1] Jing Bai,[1] Li-Min Mu,[1] Yan Yan,[1] Jia-Lun Duan,[1] Yi-Nuo Cui,[1] Zhan-Bo Su,[1] Ying Xie,[1] and Wan-Liang Lu[1]

[1]State Key Laboratory of Natural and Biomimetic Drugs, Beijing Key Laboratory of Molecular Pharmaceutics and New Drug System, and School of Pharmaceutical Sciences, Peking University, Beijing, China

Relapse of cancer is associated with multidirectional differentiation and unrestricted proliferative replication potential of cancer stem cells. Herein, we propose the plastic differentiation strategy for irreversible differentiation of cancer stem cells; further, salinomycin and its newly constructed functional liposomes are used to implement this strategy. Whole gene, cancer stem cell-related RNA, and protein expression analyses reveal that salinomycin induces the cancer stem cells into normal cells, dormant cells, and mature cancer cells. Besides, the results indicate that the gatekeeper is related to the inhibition of the protein kinase C (PKC) α signaling pathway. The differentiated normal or dormant cells are incorporated into normal tissue, whereas the rest are killed by chemotherapy. The findings would offer the evidence for plastic differentiation of cancer stem cells and propose a novel strategy for cancer therapy.

INTRODUCTION

Evidence shows that the occurrence, development, and relapse of cancer after treatment are related to a small number of cell subpopulations.[1,2] These cells are referred to as cancer stem cells (CSCs), which have self-renewal, infinite proliferation and differentiation potential. They can not only generate new CSCs but also differentiate into mature cancer cells.[3] CSCs play a decisive role in the formation, development, and metastasis of the tumor.[4]

The existing strategies by a comprehensive treatment of tumors are not effective because of the relapse from CSCs. For instance, surgical operation is unable to remove all of the surrounding tissues of cancer, whereas the residual CSCs can regenerate new cancer cells. Furthermore, treatments of regular chemotherapy and radiation cannot eliminate CSCs as well, due to multidrug resistance and radiation resistance.[5–8] These are because CSCs are often at rest and rarely divide or proliferate. Cell-cycle-specific drugs are only sensitive to cancer cells at certain phases of the proliferation cycle, such as cytarabine acting on the cells at S phase and vincristine acting on the cells at M phase, but insensitive to CSCs usually at the G0 phase. Consequently, many anticancer drugs cannot effectively treat CSCs.[9] Besides, CSCs can also activate radiation-responsive DNA damage checkpoints, and they repair radiation-induced DNA damage more efficiently than cancer cells do.[10–12] Therefore, how to eliminate CSCs remains to be the important scientific and clinical issues.

In this study, we proposed a new plastic differentiation strategy for cancer therapy. Plasticity and elasticity are a pair of antonyms, and accordingly, we define that the plastic differentiation is a kind of non-rebound and irreversible differentiation. Here, CSC plastic differentiation refers to the process by which CSCs (initiating cells) divide and differentiate into normal cells, dormant cells, and mature cancer cells. The plastically differentiated normal cells or dormant cells could be incorporated into a normal part of body tissue, whereas the differentiated cancer cells could be killed by the treatment with chemotherapy drugs during the same process.

The objectives of the study are to treat CSCs by inducing the plastic differentiations. We constructed a new kind of functional drug liposomes by incorporating distearylphosphatidyl ethanolamine polyethylene glycol-peptide-3 (DSPE-$PEG_{2,000}$-Pep-3) on the surface of liposomes as the functional molecule and by encapsulating salinomycin as the differentiation-inducing agent. The functional paclitaxel liposomes were similarly fabricated as the anticancer drug.

Pep-3 is a member of amphiphilic transmembrane peptides with a polypeptide chain of 15 amino acids (Ac-KWFETWFTEWPKKRK-OH) and with binding region and uptake region.[13] DSPE-$PEG_{2,000}$ is a pegylated derivative of the lipid, which enables the circulation effect of drug carriers in the blood system by avoiding the rapid elimination of the reticuloendothelial system (RES). Accordingly, engineered surface modification of drug liposomes with DSPE-$PEG_{2,000}$-Pep-3 is beneficial

Received 9 June 2020; accepted 27 July 2020;
https://doi.org/10.1016/j.omto.2020.07.009.

[2]These authors contributed equally to this work.

Correspondence: Wan-Liang Lu, PhD, School of Pharmaceutical Sciences, Peking University, Beijing 100191, China.
E-mail: luwl@bjmu.edu.cn
Correspondence: Ying Xie, PhD, School of Pharmaceutical Sciences, Peking University, Beijing 100191, China.
E-mail: bmuxieying@bjmu.edu.cn

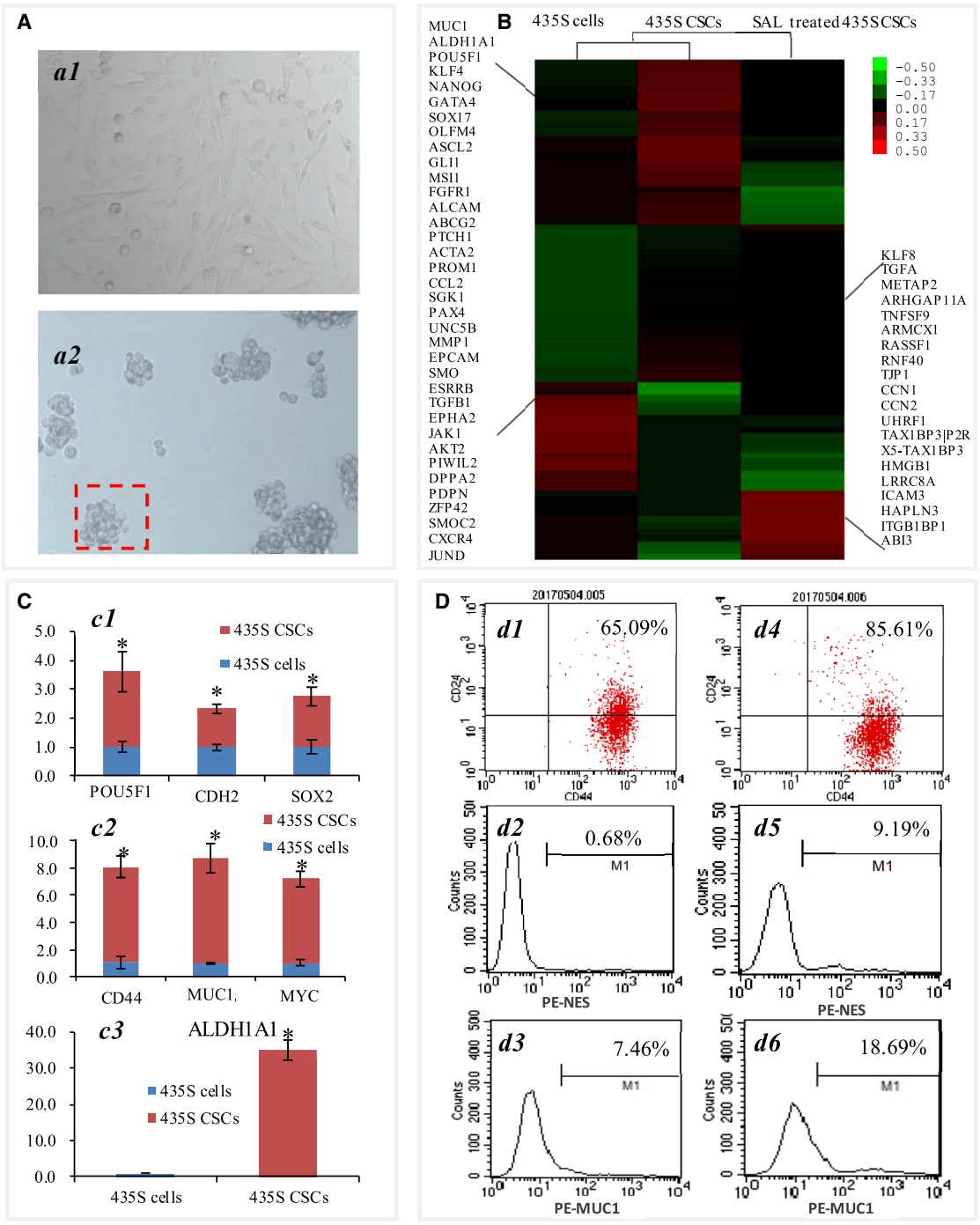

Figure 1. Identification of MDA-MB-435S Breast Cancer Stem Cells (435S CSCs)

(A) Microscopic images showing the appearance of 435S CSC during the inducing process (a1: Day 1; a2: Day 6). (B) Gene-expression microarray showing the differential gene expressions among MDA-MB-435S breast cells (435S cells), 435S CSCs, and plastically differentiated cells from 435S CSCs (salinomycin [SAL]-treated 435S CSCs). (C) Expression ratios of stem cell-related genes in 435S cells and in 435S CSCs. The results were measured by qPCR. *$p < 0.05$ versus 435S cells. Data are presented as mean ± standard deviation (n = 3). (D) Identification of phenotypes for the CSCs by FACScan flow cytometer. 435S cells were stained with anti-CD44-FITC, anti-CD24-PE (d1), anti-NES-PE (d2), and anti-MUC1-PE antibodies (d3); 435S CSCs were stained with anti-CD44-FITC, anti-CD24-PE (d4), anti-NES-PE (d5), and anti-MUC1-PE antibodies (d6).

to enhance the accumulation of drug liposomes in the tumor site and to increase phagocytosis of the drug liposomes by cancer cells. Besides, as an antimicrobial drug, salinomycin mainly acts as an ionophore in promoting the transport of cations (K^+, Na^+, Ca^{2+}, or Mg^{2+}) across the cell membrane. Recent studies have shown that salinomycin has the potential to treat cancer and CSCs. Salinomycin can activate nontraditional cell death pathways; increase DNA damage;[14,15] and inhibit tumor migration, invasion, proliferation, and epithelial-mesenchymal transition (EMT) by regulating Smad, Wnt,[16] and Hedgehog pathways.[17–19]

The experiments were mainly performed on MDA-MB-435S breast cancer cells (hereafter referred to as 435S cells) and their stem cells. 435S cells were originally isolated from the pleural fluid of a 31-year-old female patient with metastatic mammary duct adenocarcinoma, but they were contaminated with M14 melanoma cells. These unique cancer cells lead to their more tolerant nature to chemotherapy and radiotherapy and hence, were included in this investigation. In part of experiments, MDA-MB-231 breast cancer cells (hereafter referred to as 231 cells) and MCF-7 breast cancer cells (MCF-7 cells) were also included, and both were derived from the pleural effusion of a 51-year-old female patient with metastatic breast cancer and from the pleural effusion of a 69-year-old female patient with metastatic breast cancer, respectively. This study provides a theoretical basis and lays an experimental foundation for revealing the plastic differentiation treatment of CSCs, indicting scientific significance and potential clinical application value.

RESULTS

Identification of CSCs

To isolate and culture the CSCs *in vitro*, we used the serum-free suspension culture method by adding specific growth factors, consisting of epidermal growth factor (EGF), basic fibroblast growth factor (bFGF), insulin, bovine serum albumin (BSA), and B27 supplement in DMEM-Ham's F12 culture medium.[1,20–22] We acquired MCF-7 breast CSCs (hereafter referred to as MCF-7 CSCs) and MDA-MB-435S breast CSCs (hereafter referred to as 435S CSCs). Figures 1A and S1A showed the appearance of CSCs cultured in serum-free medium for 6 days. On the first day of induction, there was a small amount of cells adhered to the wall. After 6 days of induction, the number of cells was increased, and they aggregated into mammospheres.

To identify the stemness in the mammospheres after 1 week of serum-free suspension culture, we evaluated the gene and protein biomarkers of the cells by gene-expression microarray, qRT-PCR, and flow cytometry.

The gene-expression microarray results (Figure 1B) demonstrated that the expressions of traditional stem cell-related genes in the induced 435S cells were enhanced (e.g., *MUC1* [*CA 15-3*], *ALDH1A1*, *POU5F1* , *KLF4*, and *NANOG*), and genes related to invasiveness were upregulated (e.g., *OLFM4* and *CXCR4*), whereas the expressions of genes associated with cell adhesion were decreased.

Besides, we detected the difference in expression of some specific stem cell-related RNA in the induced cancer cells. The results showed that *CD44*, *MUC1*, and *POU5F1* increased 17.09 ± 7.14, 2.95 ± 0.19, and 3.23 ± 0.59 times, respectively, in the induced MCF-7 cells (Figure S1B), and *ALDH1A1*, *CD44*, *MUC1*, *CDH2*, *MYC*, *SOX2*, and *POU5F1* increased 35.14 ± 2.75, 7.01 ± 0.79, 7.74 ± 1.11, 1.32 ± 0.16, 6.18 ± 0.61, 1.74 ± 0.33, and 2.60 ± 0.69 times, respectively, in the induced 435S cells (Figure 1C).

To further identify the phenotypes of the induced cancer cells, we analyzed the protein expressions on the surface of the cells by flow cytometry. We found that the expressions of CD44+/CD24−, NES+, and MUC1+ were all elevated in the induced MCF-7 cells (Figure S1C) and in the induced 435S cells (Figure 1D). These results illustrated that the cancer cells were induced into CSCs after being cultured in serum-free medium for 1 week.

Characterization of Liposome Formulations

To increase the uptake and targeting ability of drugs, we synthesized and characterized a new functional molecule, DSPE-$PEG_{2,000}$-Pep-3 (Figure S2), followed by constructing a new kind of functional drug liposome by incorporating the molecule onto the surface of liposomes. The various liposome formulations were characterized before performing experiments on the cells and mice (Table S1). The liposome vesicles were all dispersed stably, whereas the functional salinomycin liposomes had better uniformity and stronger drug-loading capacity. Zeta potential values were approximately electrically neutral.

Plastic Differentiation of CSCs Induced by Salinomycin

To investigate the mechanism concerning how much amount of salinomycin differentiated the CSCs, we set MCF-7 CSCs and 435S CSCs as the models and analyzed the expression differences in genes and in proteins of the CSCs after being treated with salinomycin for 24 h.

At first, to make sure that it was the differentiation that caused the changes in the expression of genes or proteins, we evaluated the cytotoxicity of free salinomycin and its liposome formulations. Figure 2A illustrated the inhibitory effects on the MCF-7 CSCs and 435S CSCs after being treated with salinomycin. The results showed that free salinomycin, salinomycin liposomes, and functional salinomycin liposomes had no significant killing effect on CSCs at low doses ($\leq$0.5 μM).

The gene-expression microarray (Figure 1B) revealed that there were plenty of stem cell-related or cancer cell-associated genes significantly downregulated, whereas the genes associated with cell adhesion were significantly upregulated in 435S CSCs after being treated with salinomycin. As depicted in the gene heatmap, the *TGFA* gene and *METAP2* gene, which were overexpressed in cancer cells, were decreased, indicating that some of the CSCs were differentiated into normal cells.[23–27] The expressions of cancer-suppressing genes, including *ARHGAP11A*, *TNFSF9*, *ARMCX1*, *RASSF1*, and *RNF40*, were elevated, implying that some of the CSCs were differentiated into normal cells or dormant cells.[28,29] In addition, the expression

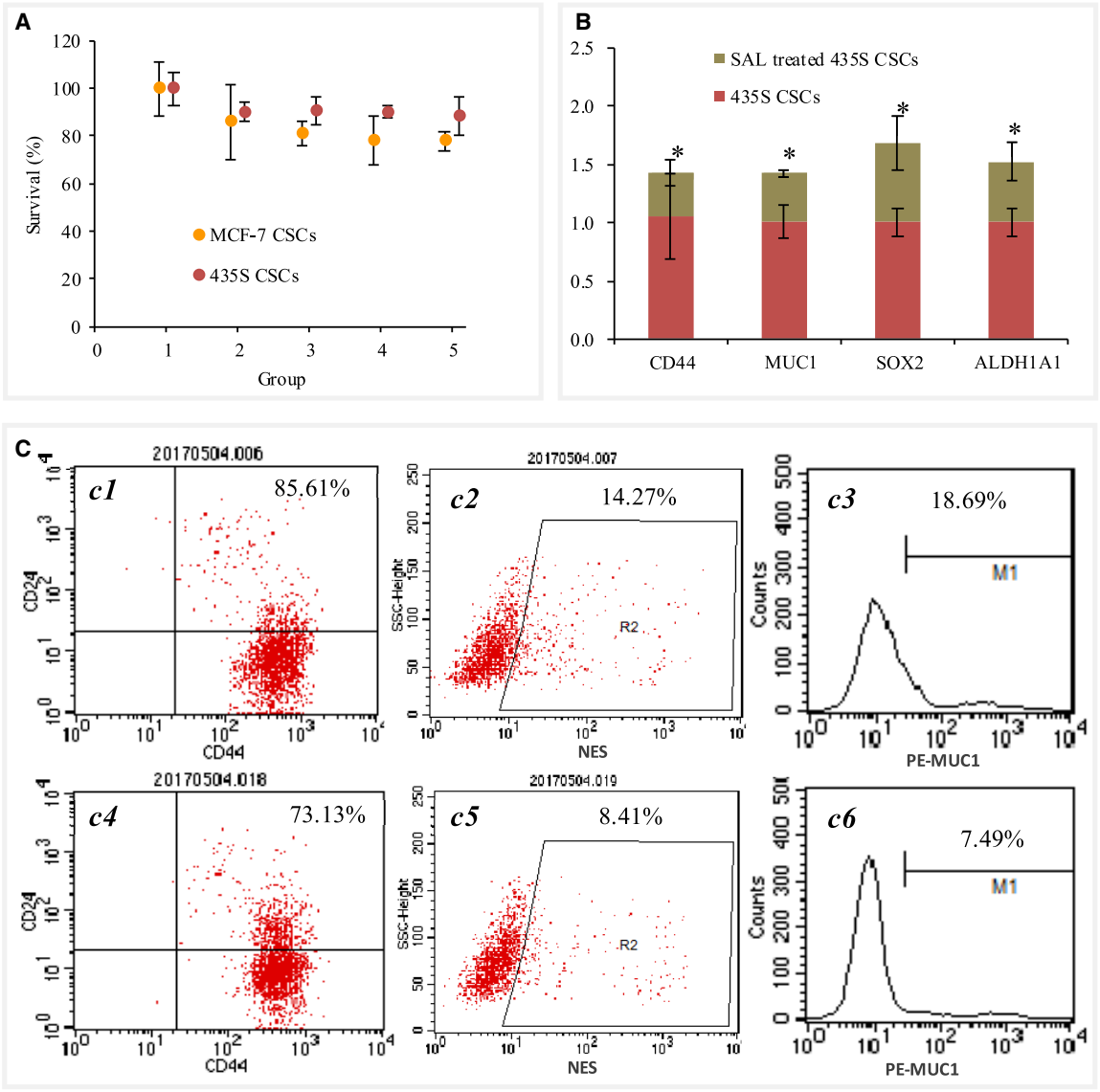

Figure 2. Plastic Differentiation of MDA-MB-435S Breast Cancer Stem Cells (435S CSCs) Induced by SAL

(A) Inhibitory effects to CSCs after treatment with SAL for 24 h. 1, treated with blank; 2, treated with 0.25 μM-free SAL; 3, treated with 0.5 μM-free SAL; 4, treated with 0.25 μM SAL liposomes; 5, 0.25 μM functional SAL liposomes. (B) Expression ratios of stem cell-related genes in 435S CSCs and in plastically differentiated cells from 435S CSCs after being treated with SAL for 24 h (SAL-treated 435S CSCs). The results were measured by qPCR. *$p < 0.05$ versus 435S CSCs. Data are presented as mean ± standard deviation (n = 3). (C) Identification of phenotypes for the differentiated cells by FACScan flow cytometer. 435S CSCs were stained with anti-CD44-FITC, anti-CD24-PE (c1), anti-NES-PE (c2), and anti-MUC1-PE antibodies (c3); SAL-treated 435S CSCs were stained with anti-CD44-FITC, anti-CD24-PE (c4), anti-NES-PE (c5), and anti-MUC1-PE antibodies (c6).

levels of cell adhesion and differentiation-related genes, such as *TJP1* and *ICAM3*, were increased.[30,31] These results verified that salinomycin could induce CSCs into normal cells, dormant cells, and mature cancer cells.

To further study the differentiation effect on RNA of the CSCs, we detected the expressions of a certain stem cell-related RNA. After being treated with salinomycin, the expression of *POU5F1* decreased to 0.36 ± 0.05 times, whereas the expressions of *SOX2*, *CDH2*, *MUC1*, and *MYC* increased 1.27 ± 0.23, 1.37 ± 0.05, 1.60 ± 0.27, and 2.52 ± 0.28 times, respectively, in the plastically differentiated MCF-7 CSCs (Figure S3A). Similarly, after being treated with salinomycin, the expressions of *CD44*, *MUC1*, *SOX2*, and *ALDH1A1* decreased to 0.37 ± 0.11, 0.41 ± 0.04, 0.68 ± 0.23, and 0.52 ± 0.16 times, respectively, in plastically differentiated 435S CSCs (Figure 2B). These results implied that

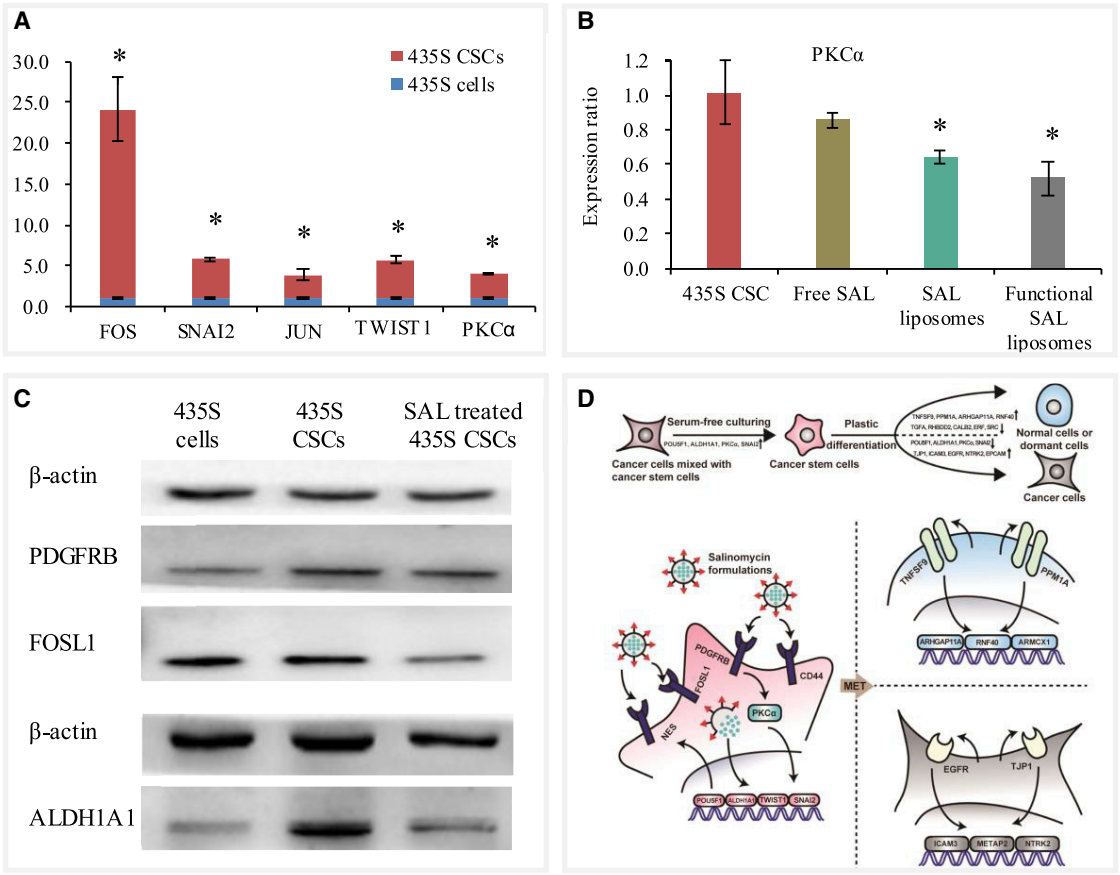

Figure 3. Blockage of PKCα Signaling Pathway in MDA-MB-435S Breast Cancer Stem Cells (435S CSCs)

(A) Expression ratios of PKCα pathway marker in MDA-MB-435S breast cancer cells (435S cells) and in 435S CSCs. The results were measured by qPCR. *$p < 0.05$ versus 435S cells. Data are presented as mean ± standard deviation (n = 3). (B) Expression ratios of PKCα pathway marker in 435S CSCs and in plastically differentiated cells from 435S CSCs, after being treated with salinomycin (SAL-treated 435S CSCs. The results were measured by qPCR. *$p < 0.05$ versus 435S CSCs. Data are presented as mean ± standard deviation (n = 3). (C) Protein expressions of PKCα pathway markers in 435S cells, 435S CSCs, and SAL-treated 435S CSCs by western blot. (D) Schematic diagram of the plastic differentiation mechanism of CSCs induced by SAL.

the CSCs were plastically differentiated by salinomycin. In addition, the results from the upregulated stem cell-related biomarkers (*SOX2*, *CDH2*, *MUC1*, and *MYC*) displayed that the CSCs were induced to normal stem cells.

Flow cytometry results (Figure S3B) revealed that the expressions of CD44+/CD24− and NES+ were decreased in the plastically differentiated MCF-7 CSCs, whereas the expression of MUC1+ was increased, demonstrating that the CSCs were differentiated, and some were induced into normal stem cells. The expressions of CD44+/CD24−, Nestin+, and MUC1+ were decreased in the plastically differentiated 435S CSCs, demonstrating that the CSCs were differentiated.

In addition, we testified whether salinomycin could induce cell-cycle arrest by flow cytometry (Table S2). The experiment was performed on 435S cells and 435S CSCs. The results showed that salinomycin could block the cell cycle of CSCs in the S phase by treating with 0.05 μM for 24 h, whereas it could block the cell cycle of CSCs in the G2/M phase after treating with 0.01, 0.25, or 0.50 μM for 24 h. The results showed that salinomycin could induce the arrest of cell cycle at different phases with a nonproportional concentration relationship, thereby leading to the dormancy of CSCs.

Blockage of Protein Kinase C (PKC) α Signaling Pathway

To investigate how salinomycin induced the plastic differentiation of CSCs, we detected the expressions of certain biomarkers of the PKCα signaling pathway by qRT-PCR. The experiments were mainly performed on MCF-7 cells, 435S cells, and their stem cells.

After being cultured in serum-free medium, the RNA expressions of *PKCα*, *TWIST1*, *JUNB*, *FOS*, and *SNAI2* were upregulated 4.51 ± 1.49, 5.60 ± 1.42, 1.98 ± 0.24, 1.23 ± 0.02, and 1.58 ± 0.14 times, respectively, in the induced MCF-7 cells (Figure S4A), and the RNA expressions of *FOS*, *SNAI2*, *JUN*, *TWIST1*, and *PKCα* were upregulated 23.15 ± 3.95, 4.78 ± 0.22, 2.86 ± 0.63, 4.71 ± 0.47, and 3.03 ± 0.21

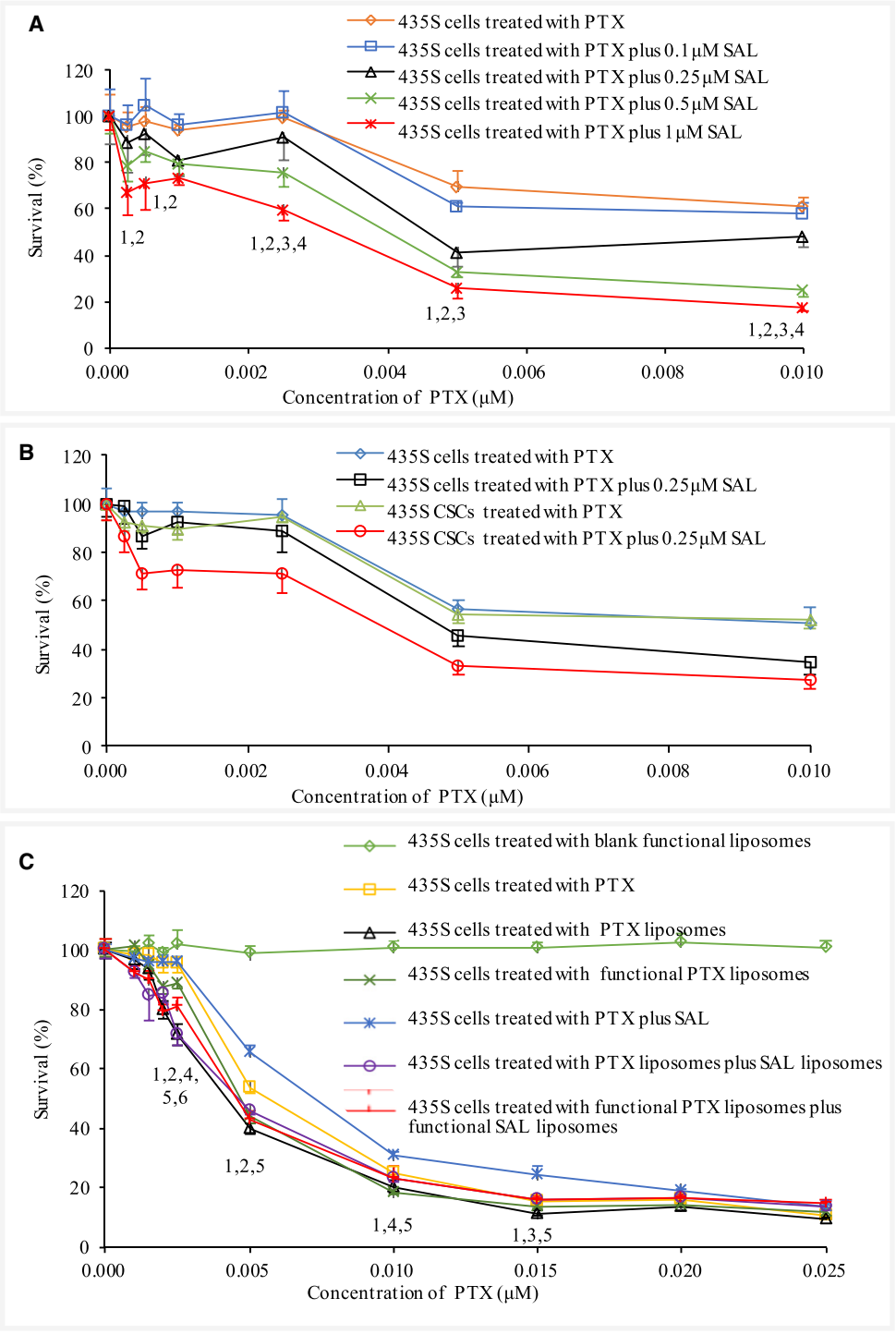

Figure 4. Enhanced Cytotoxicity by Combining Use of Functional Paclitaxel Liposomes and Functional SAL Liposomes

(A) Inhibitory effects to MDA-MB-435S breast cancer cells (435S cells) after treatment with paclitaxel (PTX) plus SAL. $p < 0.05$. 1, versus treated with PTX; 2, versus treated with PTX plus 0.1 μM SAL; 3, versus treated with PTX plus 0.25 μM SAL; 4, versus treated with PTX plus 0.5 μM SAL. Data are presented as mean ± standard deviation (n = 6).

(legend continued on next page)

times, respectively, in the induced 435S cells (Figure 3A). These results indicated that the serum-free suspension culturing could activate the PKC α signaling pathway, inducing the cancer cells into CSCs.

When CSCs were treated with salinomycin for 24 h, the RNA expressions of *PKCα*, *TWIST1*, *FOS*, and *JUNB* were downregulated to 0.47 ± 0.06, 0.71 ± 0.06, 0.86 ± 0.12, and 0.79 ± 0.06 times, respectively, whereas the RNA expression of *JUN* was upregulated 1.58 ± 0.40 times in the differentiated cells as compared to MCF-7 CSCs (Figure S4B). Besides, when being treated with free salinomycin, salinomycin liposomes, and functional salinomycin liposomes, the RNA expressions of *PKCα* were downregulated to 0.86 ± 0.05, 0.65 ± 0.04, and 0.52 ± 0.10 times in the differentiated cells, respectively, as compared to 435S CSCs (Figure 3B). The results revealed that salinomycin could block the PKC α signaling pathway, thereby inducing the plastic differentiation in CSCs. The functional salinomycin liposomes had a better inhibiting effect. In addition, the results from the upregulated stem cell-related biomarker (*JUN*) displayed that the CSCs were induced to normal stem cells.

The results from western blot (Figure 3C) also showed that the expressions of the biomarkers in the PKC α signaling pathway, platelet derived growth factor receptor beta (PDGFRB), FOSL1, and the stem cell-related biomarker, ALDHA1, were increased after being cultured in serum-free medium for 1 week and decreased after being treated with salinomycin for 24 h, which reconfirmed the theory stated above.

Enhancement in Cytotoxicity

To evaluate whether the plastic differentiation therapy could enhance the efficacy in suppressing the cancer cells and CSCs, we performed inhibitory analysis on MCF-7 cells, 435S cells, and 231 cells.

The results (Figures 4A and S5A) showed that the inhibitory effect of paclitaxel was significantly enhanced when applying paclitaxel plus salinomycin on MCF-7 cells, 435S cells, and 231 cells, especially at low concentrations of paclitaxel (≤0.01 μM). Besides, the inhibitory effect of paclitaxel to the cancer cells was elevated with the increase of salinomycin concentration, showing a dose-dependent manner. The inhibitory effect of salinomycin alone was minimal until its concentration was increased up to 0.25 μM. Therefore, 0.25 μM salinomycin was selected as the inducing plastic differentiation concentration (Figure S5B). Consequently, the inhibitory effect of serial concentrations of paclitaxel (0–0.01 μM), with a fixed concentration of 0.25 μM salinomycin, was further evaluated on 435S cells and 435S CSCs (Figure 4B). The results exhibited that, when applying low concentrations of paclitaxel (≤0.0025 μM), the inhibitory effect on both of cancer and CSCs was negligible. When applying a combination of paclitaxel (≤0.0025 μM) with 0.25 μM salinomycin, the inhibitory effect was significantly increased on the CSCs but minimal on the cancer cells.

The inhibitory effects of liposome drug formulations were evaluated on MCF-7 cells (Figure S5C) and 435S cells (Figure 4C), and the results showed that the functional blank liposomes or the salinomycin liposomes had no obvious cytotoxicity to both cells, demonstrating that salinomycin, blank liposomes, and functional material DSPE-$PEG_{2,000}$-Pep-3 were not toxic to the cancer cells. When applying the combination of functional paclitaxel liposomes and functional salinomycin liposomes, the treatment indicated a significant killing effect to both cancer cells.

Enhancement in Anticancer Efficiency *In Vivo*

To evaluate the treatment efficacy by plastic differentiation, the study was performed on the 435S cell xenografted tumor model in nude mice (Figure 5A). The results showed that the tumor inhibition rate for free paclitaxel was 18.86 ± 8.66%, the tumor inhibition rate for paclitaxel liposomes was 11.05 ± 6.18%, the tumor inhibition rate for functional paclitaxel liposomes was 15.54 ± 7.09%, and the tumor inhibition rate for the combination therapy of functional paclitaxel liposomes with functional salinomycin liposomes was 37.12 ± 5.28% after drug administrations for 10 days.

To preliminarily evaluate the safety of the formulations, we monitored the body weight of each mouse during drug administrations. The results (Figure 5B) showed that the body weight of each mouse was not evidently decreased during administrations for all drug formulations as compared to the blank control.

To verify the plastic differentiation effect of salinomycin in animals, we tested the gene-expression differences in the tumors after drug administrations with physiological saline, free salinomycin, salinomycin liposomes, and functional salinomycin liposomes for 10 days, respectively. The results (Figure 5C) demonstrated that the expressions of stem cell-related genes were decreased (e.g., *JUN*, *TWIST2*, *FOSL1*, *FOS*, *NANOG*, and *MUC1*), whereas the expressions of the cell adhesion-associated or differentiation-associated genes were increased (e.g., *TJP1*, *EPCAM*, and epidermal growth factor receptor [*EGFR*]).

Besides, the expressions of cancer cell-related genes were decreased (e.g., *TGFA*, *RHBDD2*, *MIEN1*, *CST7*, and *CTAG2*), whereas the expressions of cancer-suppressing genes were elevated (e.g., *FABP3*, *ARMCX1*, *STK11*, *ARHGAP11A*, and *RNF40*). Furthermore, the expressions of normal stem cell-related genes were upregulated as well (e.g., *ITGB1*, *ITGA6*, and *PECAM1*). These results implied that the CSCs in tumors were differentiated into normal cells, dormant cells, and mature cancer cells.

DISCUSSION

Previous studies have shown that both small-molecule drugs (all-trans retinoic acid[32] and cinnamate[33]) and macromolecule agents (bone

(B) Inhibitory effects to 435S cells and MDA-MB-435S breast cancer stem cells (435S CSCs) after treatment with PTX plus SAL. (C) Inhibitory effects to 435S cells after treatment with PTX, SAL, and their liposome formulations. $p < 0.05$. 1, versus treated with blank functional liposomes; 2, versus treated with PTX; 3, versus treated with PTX liposomes; 4, versus treated with functional PTX liposomes; 5, versus treated with PTX plus SAL; 6, versus treated with PTX liposomes plus SAL liposomes. SAL in all of the formulations was fixed at 0.25 μM. Data are presented as mean ± standard deviation (n = 6).

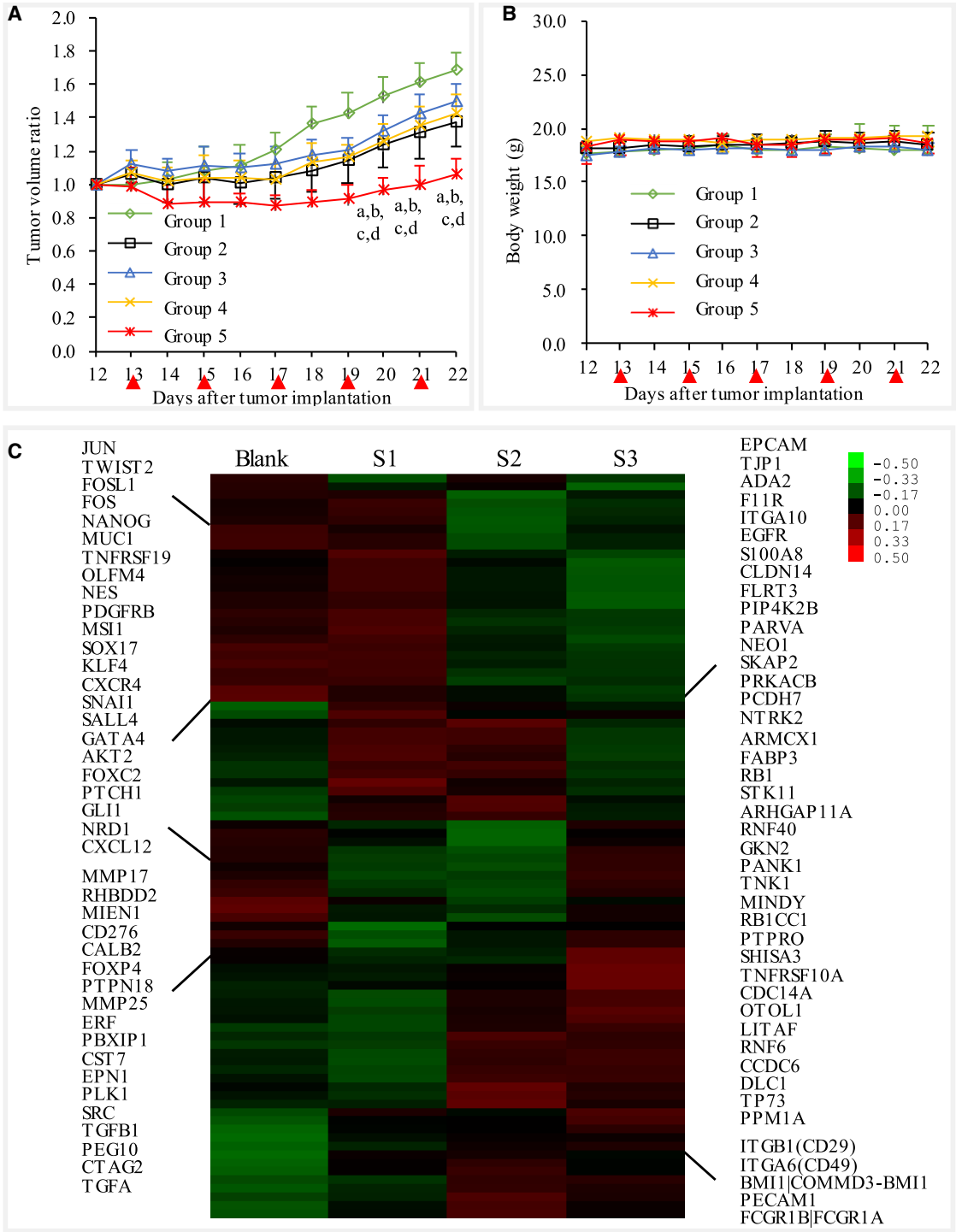

Figure 5. Enhanced Anticancer Efficiency and Induced Plastic Differentiation *In Vivo*

(A) Anticancer efficacy after treatment with varying formulations in MDA-MB-435S breast cancer cell xenografts in nude mice. Group 1, physiological saline; group 2, PTX; group 3, PTX liposomes; group 4, functional PTX liposomes; group 5, functional PTX liposomes plus functional SAL liposomes. The arrows indicate the day of drug administration. $p < 0.05$. a, versus group 1; b, versus group 2; c, versus group 3; d, versus group 4. Data are presented as mean ± standard deviation (n = 5). (B) Body weight changes during the treatment process with varying formulations in the above cancer xenografts in nude mice. Group 1,

(legend continued on next page)

morphogenetic proteins[34]) are able to induce the differentiation of CSC into mature cancer cells, whereas the differentiated mature cancer cells can be more effectively killed by anticancer drugs. In this study, we reveal that the antibiotic salinomycin can induce the differentiation of CSCs as well. Furthermore, such a differentiation could go in two directions: forward and backward. The forward differentiation leads to the transformation of CSCs into mature cancer cells, which can be more easily killed by treatment of anticancer drugs. In contrast, the backward differentiation results in the transformation of CSCs into normal or dormant cells (benign cells or sleepy cancer/normal stem cells), which are unharmful to human health.

The serum-free suspension culture method was used to acquire CSCs. Cancer cells adherently grew in serum-containing medium but not in serum-free medium, whereas CSCs could survive and proliferate as mammospheres in serum-free medium.[35–38] In this experiment, by adding B27 growth factor and increasing the frequency of medium exchange, cancer cells could be induced into CSCs in about 1 week, and the cells aggregated into spheres.

We analyzed the expression changes in RNA or protein of a variety of genes, including stem cell-related genes (e.g., *CD44+/CD24−*, *MUC1*, *ALDH1A1*, *POU5F1*, *SOX2*, and *NES*), cell adhesion and differentiation-related genes (e.g., *CDH2*), and cancer cell-related genes (e.g., *MYC*). The changes in the expression levels of these genes could reflect the type of cells, thereby verifying the generation and the induced plastic differentiation of CSCs. The gene-expression changes before and after serum-free suspension culture demonstrated that the cancer cells were successfully induced into CSCs, thus providing the experimental materials for the study of plastic differentiation. The gene-expression changes before and after being treated with salinomycin for 24 h implied that the CSCs were plastically differentiated into normal cells, dormant cells, and mature cancer cells. The experiments on tolerance concentration of salinomycin to CSCs indicated that the decreases in stem cell-related markers and cancer cell-related factors were not related to the death of the cells but derived from the plastic differentiation of CSCs induced by salinomycin.

PKCα is one of the protein kinase families that has at least ten subtypes (α, βI, βII, γ, δ, ε, η, θ, ζ, and ι). Studies showed that the increased expression of PKCα could promote the metastasis of cancer cells.[39] PKCα was a central signal pathway and therapeutic target for CSCs, whereas inhibition of PKCα had a strong effect on CSCs. Therefore, to explain the mechanism of the plastic differentiation, the key biomarkers in RNA and protein levels in the PKCα signaling pathway were analyzed.

After serum-free suspension culture, PKCα was activated by growth factors.[39,40] PKCα induced the expression of *SNAI1* mRNA by activating early growth response 1 (EGR1),[40] and the transcription factor *TWIST1* was also activated. *FOSL1*, the transcriptional target of *SNAI1* and *TWIST1*, was phosphorylated and associated with members of the *JUN* family of transcription factors to form heterodimeric activator protein-1 (AP-1) complexes, leading to the EMT. In the process, a shift from EGFR to PDGFR signaling occurred. Then, *PKCα* was further activated, and extracellular regulated MAP kinase (Erk) signaling was also elevated, which together, led to further accumulation of phosphorylated *FOSL1*.[41] The results from the increased expressions of stem cell-related biomarkers (such as *POU5F1*, *ALDH1A1*, and *SNAI2*) indicated that the cancer cells were induced into CSCs by serum-free suspension culture.

After being treated with salinomycin and its liposome formulations, the PKCα signaling pathway in the CSCs was blocked, and this blockage led to the inhibition of PKCα-dependent activation of *FOSL1*, resulting in the occurrence of mesenchymal-epithelial transition (MET).[41] The plastic differentiation resulted in a forward and a backward transition: benign differentiation and malignant transformation.

The occurrence of benign differentiation was associated with the following factors: the downregulation of cell proliferation-related genes (*TGFA*, *ERF*, and *SRC*) and cell migration-related genes (*MIEN1* and *SRC*), as well as the upregulation of cancer-suppressing genes (*ARHGAP11A*, *TNFSF9*, *ARMCX1*, *RASSF1*, *PPM1A*, and *RNF40*). As a result, CSCs differentiated into normal cells or dormant cells. The downregulated cancer cell-related markers (*RHBDD2*, *CALB2*, *CST7*, and *METAP2)* further confirmed the benign differentiation. On the contrary, with the shift from PDGFR to EGFR signaling, part of CSCs went in malignant transformation. This could be explained by the facts that cell adhesion-related genes (*TJP1* and *ICAM3*) and stem cell differentiation-related genes (*NTRK2* and *EPCAM*) were upregulated, whereas stem cell-related biomarkers (*CD44*, *POU5F1*, *ALDH1A1*, and *SNAI2*) were downregulated. Eventually, the CSCs turned into mature cancer cells (Figure 3D).

The aim of plastic differentiation was to provide a new strategy on eliminating CSCs. Accordingly, the anticancer efficiency of salinomycin was evaluated when it was used alone or in combination with an anticancer drug. *In vitro* and *in vivo* experiments both exhibited that the combination of functional paclitaxel liposomes and functional salinomycin liposomes had a significant killing effect to breast cancer cells. This could be explained by a mechanism that salinomycin induced the plastic differentiation of CSCs into normal cells, dormant cells, and mature cancer cells, and then the differentiated normal cells or dormant cells could be incorporated into normal tissue, whereas the rest of cancer cells could be killed by chemotherapy during the same process. The study may reflect the anticancer efficacy for a new plastic differentiation-based strategy.

physiological saline; group 2, PTX; group 3, PTX liposomes; group 4, functional PTX liposomes; group 5, functional PTX liposomes plus functional SAL liposomes. The arrows indicate the day of drug administration. Data are presented as mean ± standard deviation (n = 5). (C) Gene-expression microarray showing the differential gene expressions of the tumor tissues after being treated with physiological saline (Blank), free SAL (S1), SAL liposomes (S2), and functional SAL liposomes (S3).

In conclusion, we proposed a new scientific concept on plastic differentiation of CSCs. Whole gene analysis revealed the changes in major stem cell-related genes during plastic differentiation. The upregulated cancer-suppressing genes (*ARHGAP11A*, *TNFSF9*, *ARMCX1*, *RASSF1*, *PPM1A*, and *RNF40*) and downregulated cancer cell-related genes (*TGFA*, *RHBDD2*, *CALB2*, *ERF*, *SRC*, *MIEN1*, *CST7*, and *METAP2*) indicated the benign differentiation in forming normal or dormant cells, whereas the downregulated stem cell-related genes (*CD44*, *POU5F1*, *ALDH1A1*, *PKCα*, and *SNAI2*) and the upregulated differentiation and cell adhesion-related genes (*TJP1*, *ICAM3*, *EGFR*, *NTRK2*, and *EPCAM*) denoted the malignant differentiation in producing mature cancer cells. Besides, we found that the gatekeeper for plastic differentiation is related to the blockage of the PKCα signaling pathway. This study may offer a novel treatment strategy for treatment of cancer and CSCs, hence having an important scientific significance and potential clinical application value.

MATERIALS AND METHODS

Key resource information was listed in Table S3 of the Supplemental Information.

Cell Preparation

MCF-7 cells were maintained in RPMI-1640 medium, whereas 231 cells and 435S cells were maintained in Leibovitz's L15 medium, and the two kinds of medium were both supplemented with 10% fetal bovine serum (FBS), 100 units/mL penicillin, and 100 units/mL streptomycin. MCF-7 CSCs and 435S CSCs were cultured in serum-free culture medium, as reported previously.[42] In this experiment, the insulin dosage was adjusted to 5 mg/mL, and the 0.2% B27 growth factor was added to increase the frequency of medium exchange.

Construction and Characterization of Drug Formulations

DSPE-$PEG_{2,000}$-Pep-3 conjugate was newly developed by conjugating 1,2-distearoyl-sn-glycero-3-phosphatidylethanolamine-polyethyleneglycol$_{2000}$-N-hydroxysuccinimide (DSPE-$PEG_{2,000}$-NHS) with Pep-3. Briefly, Pep-3 and DSPE-$PEG_{2,000}$-NHS were dissolved at a ratio of 1:1 (μmol/μmol) in super dry N,N dimethylformamide (DMF) with a little triethylamine, and the coupling reaction was carried out at room temperature in a light-resistant container for 24 h. Then, the reaction mixture was transferred into dialysis tubing (molecular weight cutoff [MWCO], 2,000 Da) and dialyzed against deionized water for 48 h to remove the DMF solvent and uncoupled molecules. The conjugation was confirmed by matrix-assisted laser desorption/ionization time-of-flight mass spectrometry (MALDI-TOF-MS) and stored at −20°C.

Then, six types of liposomes were fabricated, including blank liposomes, blank functional liposomes, salinomycin liposomes, paclitaxel liposomes, functional salinomycin liposomes, and functional paclitaxel liposomes.

To construct functional salinomycin liposomes, egg phosphatidylcholine (EPC), cholesterol, and DSPE-$PEG_{2,000}$-Pep-3 (EPC:CHOL:DSPE-$PEG_{2,000}$-Pep-3 = 85:10:5, μmol/μmol) and salinomycin were dissolved in chloroform and methanol ($CHCL_3$:CH_3OH = 3:1, v/v) in a pear-shaped flask. The solvent was evaporated under a vacuum with a rotary evaporator. The remaining lipid film was hydrated with deionized water in a water-bath sonicator for 1 min, followed by probe-type sonication for 6 min. The suspensions were then serially filtered through polycarbonate membranes (pore sizes 400 and 200 nm), 3 times each, to yield functional salinomycin liposomes.

To construct functional paclitaxel liposomes, EPC and DSPE-$PEG_{2,000}$-Pep-3 (EPC:DSPE-$PEG_{2,000}$-Pep-3 = 95:5, μmol/μmol) and paclitaxel were dissolved in chloroform and methanol ($CHCL_3$:CH_3OH = 3:1, v/v) in a pear-shaped flask. The synthesis method was the same as above.

To construct salinomycin liposomes and paclitaxel liposomes, the same method was used as that for functional salinomycin liposomes or functional paclitaxel liposomes, except that there was no addition of DSPE-$PEG_{2,000}$-Pep-3.

To construct blank functional liposomes, the same method was used as that for functional salinomycin liposomes, except that there was no addition of salinomycin.

To construct blank liposomes, the same method was used as that for salinomycin liposomes, except that there was no addition of salinomycin.

The mean particle sizes, polydispersity indexes (PDIs), and zeta potential values of all liposomes were measured using the Nano Series Zenith 4003 Zetasizer.

Gene-Expression Microarray

In vitro, gene-expression microarray was performed to compare the gene-expression profiles among 435S cells, 435S CSCs, and plastically differentiated cells. Three independent samples were collected. The RNA was extracted using TRIzol and used for microarray analysis.

In vivo, gene-expression microarray was performed to compare the gene-expression profiles in the isolated tumor tissues from the cancer-bearing mouse model after treatment with physiological saline (blank control), free salinomycin, salinomycin liposomes, or functional salinomycin liposomes.

Quantitative Real-Time PCR

RNA was extracted using TRIzol, and cDNA was generated using reverse transcriptase from the PrimeScript RT Master Mix (Perfect Real Time). Real-time quantitative PCR was performed using the SYBR Premix Ex Taq II (Tli RNase H Plus). PCR was performed on cDNA using specific primers. Expression levels of the target genes were normalized to the β-actin level in each sample using the 2ΔΔct method. PCR was conducted with at least three samples. Primer sequences were listed in Table S4.

Western Blot

Cells were lysed using the radio immunoprecipitation assay (RIPA) buffer. Protein extracts were run on a 10% or 15% acrylamide gel before being transferred to a polyvinylidene fluoride membrane. Membranes were blocked with 5% nonfat dried milk for 1 h and incubated with primary antibodies overnight, followed by incubation with the secondary antibodies for 1 h at room temperature. Primary antibodies used in this study were the following: anti-β-actin, anti-ALDH1A1, and anti-PDGFRB. The immunocomplexes were detected using the MiniChemi 610.

Flow Cytometry

After continuous culture in serum-free medium under 5% CO_2 at 37°C for 1 week, mammospheres were collected for phenotype identification of MCF-7 CSCs, 435S CSCs, and plastically differentiated cells. Briefly, the mammospheres were collected, enzymatically dissociated, and washed in PBS using gentle agitation. Immunostaining was performed after incubation with anti-CD44-fluorescein isothiocyanate (FITC), anti-CD24-phycoerythrin (PE), anti-MUC1-PE, anti-NES-PE, or their appropriate isotype controls for 30 min at 4°C in PBS (pH 7.4). The samples were then washed three times with cold PBS (pH 7.4) and resuspended in 300 μL cold PBS (pH 7.4). Flow cytometry was performed on a FACScan flow cytometer. Side-scatter and forward-scatter profiles were used to eliminate cell doublets.

Cell-Cycle Arrest

435S cells and 435S CSCs were cultured as stated above. Then, salinomycin (0.01 μM, 0.05 μM, 0.25 μM, or 0.5 μM) was added into the CSCs. The cells were grown at 37°C in the presence of 5% CO_2 for 24 h. After being harvested and washed, the cells were fixed with ice-cold 70% ethanol at 4°C overnight. After washing twice with ice-cold PBS (pH 7.4), the cells were incubated with RNase A (100 μg/mL) at 37°C for 30 min. DNA was stained with propidium iodide (PI; 50 μg/mL), and the cell-cycle analysis was performed on a FACScan flow cytometer.

Cytotoxicity in Cancer and CSCs

To evaluate the cytotoxic effects of varying drug liposomes, MCF-7 cells, 435S cells, and their stem cells were seeded at a density of 7.5×10^3 cells/well in 96-well culture plates and cultured for 24 h. Then, the cells were exposed to free paclitaxel, free salinomycin, and their liposome formulations. After incubation for 48 h, the cytotoxic effects were evaluated with a sulforhodamine B (SRB) colorimetric assay. Briefly, the culture medium was removed, and then the cells were fixed with trichloroacetic acid, followed by washing with deionized water and staining with SRB. Measurement was performed at 540 nm using a microplate reader. The survival rates of the cells were calculated using the following formula: survival % = (A540 nm for treated cells/A540 nm for control cells) × 100%, where A540 nm represents the absorbance value.

Animal Experimentation

BALB/c mice (initially weighing 18–20 g) were purchased from the Health Science Center of Peking University. All procedures involving the care and handing of animals were approved and supervised by the Authorities for Laboratory Animal Care of Peking University (Beijing, China).

Briefly, approximately 1×10^7 435S cells were resuspended in 200 μL of serum-free medium and injected subcutaneously into the right flanks of nude mice. When tumors reached 100–150 mm^3 in volume, mice were randomly divided into eight treatment groups (n = 5 per group). At the 13th, 15th, 17th, 19th, and 21st day after inoculation, physiological saline, free paclitaxel (5 mg/kg), free salinomycin (1 mg/kg), paclitaxel liposomes (5 mg/kg), salinomycin liposomes (1 mg/kg), functional paclitaxel liposomes (5 mg/kg), functional salinomycin liposomes (1 mg/kg), or functional paclitaxel liposomes (5 mg/kg) plus functional salinomycin liposomes (1 mg/kg) were administered to mice via tail-vein injection. The mice were then monitored, and the tumor volume was calculated according to the following formula: the tumor volume (cubic millimeters) on the nth day = length × $width^2/2$.

To confirm the plastic differentiation in tumors, the cancer-bearing mice were sacrificed at the 22nd day after drug administration, and the tumor masses were immediately removed and stored with liquid nitrogen.

Statistical Analysis

The data are represented as the means ± standard deviation. Analysis of variance (ANOVA) was used to analyze the data by SPSS software (version 20.0; IBM, Armonk, NY, USA), after which, post hoc tests with the Bonferroni correction were used for multiple comparisons between individual groups. A value of $p < 0.05$ was considered to be significant.

SUPPLEMENTAL INFORMATION

Supplemental Information can be found online at https://doi.org/10.1016/j.omto.2020.07.009.

AUTHOR CONTRIBUTIONS

J.-Y.Z. and W.-L.L. designed the project. J.-Y.Z., Q.L., and J.B. performed the plastic differentiation of CSCs. J.-Y.Z. and J.-R.X. conducted the culturing and identification of CSCs. J.-Y.Z., L.-M.M., and Y.Y. constructed the functional materials and the functional liposomes. J.-Y.Z. and J.-L.D. performed the cytotoxicity in cancer and CSCs. Y.-N.C., Z.-B.S., and Y.X. aided in animal experiments. J.-Y.Z. wrote the manuscript. W.-L.L. and Q.L. revised the manuscript. All authors reviewed the manuscript.

CONFLICTS OF INTEREST

The authors declare no competing interests.

ACKNOWLEDGMENTS

We are grateful for the grants from the National Natural Science Foundation of China (grant number 81673367) and the Beijing Natural Science Foundation (Key Grant number 7181004).

REFERENCES

1. Ponti, D., Costa, A., Zaffaroni, N., Pratesi, G., Petrangolini, G., Coradini, D., Pilotti, S., Pierotti, M.A., and Daidone, M.G. (2005). Isolation and in vitro propagation of tumorigenic breast cancer cells with stem/progenitor cell properties. Cancer Res. *65*, 5506–5511.
2. Pardal, R., Clarke, M.F., and Morrison, S.J. (2003). Applying the principles of stem-cell biology to cancer. Nat. Rev. Cancer *3*, 895–902.
3. Reya, T., Morrison, S.J., Clarke, M.F., and Weissman, I.L. (2001). Stem cells, cancer, and cancer stem cells. Nature *414*, 105–111.
4. Dalerba, P., Cho, R.W., and Clarke, M.F. (2007). Cancer stem cells: models and concepts. Annu. Rev. Med. *58*, 267–284.
5. Chen, D., Wu, M., Li, Y., Chang, I., Yuan, Q., Ekimyan-Salvo, M., Deng, P., Yu, B., Yu, Y., Dong, J., et al. (2017). Targeting BMI1^{+} Cancer Stem Cells Overcomes Chemoresistance and Inhibits Metastases in Squamous Cell Carcinoma. Cell Stem Cell *20*, 621–634.e6.
6. Burger, H., van Tol, H., Boersma, A.W., Brok, M., Wiemer, E.A., Stoter, G., and Nooter, K. (2004). Imatinib mesylate (STI571) is a substrate for the breast cancer resistance protein (BCRP)/ABCG2 drug pump. Blood *104*, 2940–2942.
7. Houghton, P.J., Germain, G.S., Harwood, F.C., Schuetz, J.D., Stewart, C.F., Buchdunger, E., and Traxler, P. (2004). Imatinib mesylate is a potent inhibitor of the ABCG2 (BCRP) transporter and reverses resistance to topotecan and SN-38 in vitro. Cancer Res. *64*, 2333–2337.
8. Rich, J.N. (2007). Cancer stem cells in radiation resistance. Cancer Res. *67*, 8980–8984.
9. Nguyen, P.D., Gurevich, D.B., Sonntag, C., Hersey, L., Alaei, S., Nim, H.T., Siegel, A., Hall, T.E., Rossello, F.J., Boyd, S.E., et al. (2017). Muscle Stem Cells Undergo Extensive Clonal Drift during Tissue Growth via Meox1-Mediated Induction of G2 Cell-Cycle Arrest. Cell Stem Cell *21*, 107–119.e6.
10. Ch'ang, H.J., Maj, J.G., Paris, F., Xing, H.R., Zhang, J., Truman, J.P., Cardon-Cardo, C., Haimovitz-Friedman, A., Kolesnick, R., and Fuks, Z. (2005). ATM regulates target switching to escalating doses of radiation in the intestines. Nat. Med. *11*, 484–490.
11. Wang, J., Sun, Q., Morita, Y., Jiang, H., Gross, A., Lechel, A., Hildner, K., Guachalla, L.M., Gompf, A., Hartmann, D., et al. (2012). A differentiation checkpoint limits hematopoietic stem cell self-renewal in response to DNA damage. Cell *148*, 1001–1014.
12. Bao, S., Wu, Q., McLendon, R.E., Hao, Y., Shi, Q., Hjelmeland, A.B., Dewhirst, M.W., Bigner, D.D., and Rich, J.N. (2006). Glioma stem cells promote radioresistance by preferential activation of the DNA damage response. Nature *444*, 756–760.
13. Morris, M.C., Gros, E., Aldrian-Herrada, G., Choob, M., Archdeacon, J., Heitz, F., and Divita, G. (2007). A non-covalent peptide-based carrier for in vivo delivery of DNA mimics. Nucleic Acids Res. *35*, e49.
14. Kim, J.H., Chae, M., Kim, W.K., Kim, Y.J., Kang, H.S., Kim, H.S., and Yoon, S. (2011). Salinomycin sensitizes cancer cells to the effects of doxorubicin and etoposide treatment by increasing DNA damage and reducing p21 protein. Br. J. Pharmacol. *162*, 773–784.
15. Al Dhaheri, Y., Attoub, S., Arafat, K., Abuqamar, S., Eid, A., Al Faresi, N., and Iratni, R. (2013). Salinomycin induces apoptosis and senescence in breast cancer: upregulation of p21, downregulation of survivin and histone H3 and H4 hyperacetylation. Biochim. Biophys. Acta *1830*, 3121–3135.
16. Lu, D., Choi, M.Y., Yu, J., Castro, J.E., Kipps, T.J., and Carson, D.A. (2011). Salinomycin inhibits Wnt signaling and selectively induces apoptosis in chronic lymphocytic leukemia cells. Proc. Natl. Acad. Sci. USA *108*, 13253–13257.
17. Kusunoki, S., Kato, K., Tabu, K., Inagaki, T., Okabe, H., Kaneda, H., Suga, S., Terao, Y., Taga, T., and Takeda, S. (2013). The inhibitory effect of salinomycin on the proliferation, migration and invasion of human endometrial cancer stem-like cells. Gynecol. Oncol. *129*, 598–605.
18. Zhang, C., Lu, Y., Li, Q., Mao, J., Hou, Z., Yu, X., Fan, S., Li, J., Gao, T., Yan, B., et al. (2016). Salinomycin suppresses TGF-β1-induced epithelial-to-mesenchymal transition in MCF-7 human breast cancer cells. Chem. Biol. Interact. *248*, 74–81.
19. Lu, Y., Ma, W., Mao, J., Yu, X., Hou, Z., Fan, S., Song, B., Wang, H., Li, J., Kang, L., et al. (2015). Salinomycin exerts anticancer effects on human breast carcinoma MCF-7 cancer stem cells via modulation of Hedgehog signaling. Chem. Biol. Interact. *228*, 100–107.
20. Beck, S., Jin, X., Yin, J., Kim, S.H., Lee, N.K., Oh, S.Y., Jin, X., Kim, M.K., Kim, E.B., Son, J.S., et al. (2011). Identification of a peptide that interacts with Nestin protein expressed in brain cancer stem cells. Biomaterials *32*, 8518–8528.
21. Strojnik, T., Røsland, G.V., Sakariassen, P.O., Kavalar, R., and Lah, T. (2007). Neural stem cell markers, nestin and musashi proteins, in the progression of human glioma: correlation of nestin with prognosis of patient survival. Surg. Neurol. *68*, 133–143, discussion 143–144.
22. Piras, F., Perra, M.T., Murtas, D., Minerba, L., Floris, C., Maxia, C., Demurtas, P., Ugalde, J., Ribatti, D., and Sirigu, P. (2010). The stem cell marker nestin predicts poor prognosis in human melanoma. Oncol. Rep. *23*, 17–24.
23. Shiels, M.S., Pfeiffer, R.M., Hildesheim, A., Engels, E.A., Kemp, T.J., Park, J.H., Katki, H.A., Koshiol, J., Shelton, G., Caporaso, N.E., et al. (2013). Circulating inflammation markers and prospective risk for lung cancer. J. Natl. Cancer Inst. *105*, 1871–1880.
24. Siveke, J.T., Einwächter, H., Sipos, B., Lubeseder-Martellato, C., Klöppel, G., and Schmid, R.M. (2007). Concomitant pancreatic activation of Kras(G12D) and Tgfa results in cystic papillary neoplasms reminiscent of human IPMN. Cancer Cell *12*, 266–279.
25. Selvakumar, P., Lakshmikuttyamma, A., Das, U., Pati, H.N., Dimmock, J.R., and Sharma, R.K. (2009). NC2213: a novel methionine aminopeptidase 2 inhibitor in human colon cancer HT29 cells. Mol. Cancer *8*, 65.
26. Tucker, L.A., Zhang, Q., Sheppard, G.S., Lou, P., Jiang, F., McKeegan, E., Lesniewski, R., Davidsen, S.K., Bell, R.L., and Wang, J. (2008). Ectopic expression of methionine aminopeptidase-2 causes cell transformation and stimulates proliferation. Oncogene *27*, 3967–3976.
27. Selvakumar, P., Lakshmikuttyamma, A., Dimmock, J.R., and Sharma, R.K. (2006). Methionine aminopeptidase 2 and cancer. Biochim. Biophys. Acta *1765*, 148–154.
28. Melero, I., Mazzolini, G., Narvaiza, I., Qian, C., Chen, L., and Prieto, J. (2001). IL-12 gene therapy for cancer: in synergy with other immunotherapies. Trends Immunol. *22*, 113–115.
29. Rong, R., Jiang, L.Y., Sheikh, M.S., and Huang, Y. (2007). Mitotic kinase Aurora-A phosphorylates RASSF1A and modulates RASSF1A-mediated microtubule interaction and M-phase cell cycle regulation. Oncogene *26*, 7700–7708.
30. Lee, S.W., Kim, W.J., Choi, Y.K., Song, H.S., Son, M.J., Gelman, I.H., Kim, Y.J., and Kim, K.W. (2003). SSeCKS regulates angiogenesis and tight junction formation in blood-brain barrier. Nat. Med. *9*, 900–906.
31. Shin, K., and Margolis, B. (2006). ZOning out tight junctions. Cell *126*, 647–649.
32. Sun, R., Liu, Y., Li, S.Y., Shen, S., Du, X.J., Xu, C.F., Cao, Z.T., Bao, Y., Zhu, Y.H., Li, Y.P., et al. (2015). Co-delivery of all-trans-retinoic acid and doxorubicin for cancer therapy with synergistic inhibition of cancer stem cells. Biomaterials *37*, 405–414.
33. Zajac, J., Novohradsky, V., Markova, L., Brabec, V., and Kasparkova, J. (2020). Platinum (IV) Derivatives with Cinnamate Axial Ligands as Potent Agents Against Both Differentiated and Tumorigenic Cancer Stem Rhabdomyosarcoma Cells. Angew. Chem. Int. Ed. Engl. *59*, 3329–3335.
34. Piccirillo, S.G.M., Reynolds, B.A., Zanetti, N., Lamorte, G., Binda, E., Broggi, G., Brem, H., Olivi, A., Dimeco, F., and Vescovi, A.L. (2006). Bone morphogenetic proteins inhibit the tumorigenic potential of human brain tumour-initiating cells. Nature *444*, 761–765.
35. Ricci-Vitiani, L., Lombardi, D.G., Pilozzi, E., Biffoni, M., Todaro, M., Peschle, C., and De Maria, R. (2007). Identification and expansion of human colon-cancer-initiating cells. Nature *445*, 111–115.
36. Fairbairn, L.J., Cowling, G.J., Reipert, B.M., and Dexter, T.M. (1993). Suppression of apoptosis allows differentiation and development of a multipotent hemopoietic cell line in the absence of added growth factors. Cell *74*, 823–832.
37. Leis, O., Eguiara, A., Lopez-Arribillaga, E., Alberdi, M.J., Hernandez-Garcia, S., Elorriaga, K., Pandiella, A., Rezola, R., and Martin, A.G. (2012). Sox2 expression in breast tumours and activation in breast cancer stem cells. Oncogene *31*, 1354–1365.

38. Miki, J., and Rhim, J.S. (2008). Prostate cell cultures as in vitro models for the study of normal stem cells and cancer stem cells. Prostate Cancer Prostatic Dis. *11*, 32–39.

39. Kim, J., Thorne, S.H., Sun, L., Huang, B., and Mochly-Rosen, D. (2011). Sustained inhibition of PKCα reduces intravasation and lung seeding during mammary tumor metastasis in an in vivo mouse model. Oncogene *30*, 323–333.

40. Kinehara, M., Kawamura, S., Mimura, S., Suga, M., Hamada, A., Wakabayashi, M., Nikawa, H., and Furue, M.K. (2014). Protein kinase C-induced early growth response protein-1 binding to SNAIL promoter in epithelial-mesenchymal transition of human embryonic stem cells. Stem Cells Dev. *23*, 2180–2189.

41. Tam, W.L., Lu, H., Buikhuisen, J., Soh, B.S., Lim, E., Reinhardt, F., Wu, Z.J., Krall, J.A., Bierie, B., Guo, W., et al. (2013). Protein kinase C α is a central signaling node and therapeutic target for breast cancer stem cells. Cancer Cell *24*, 347–364.

42. Zhang, L., Yao, H.J., Yu, Y., Zhang, Y., Li, R.J., Ju, R.J., Wang, X.X., Sun, M.G., Shi, J.F., and Lu, W.L. (2012). Mitochondrial targeting liposomes incorporating daunorubicin and quinacrine for treatment of relapsed breast cancer arising from cancer stem cells. Biomaterials *33*, 565–582.